Personal Authentication Using Hand Vein Triangulation and Knuckle Shape

Ajay Kumar, *Senior Member, IEEE*, and K. Venkata Prathyusha

Abstract—This paper presents a new approach to authenticate individuals using triangulation of hand vein images and simultaneous extraction of knuckle shape information. The proposed method is fully automated and employs palm dorsal hand vein images acquired from the low-cost, near infrared, contactless imaging. The knuckle tips are used as key points for the image normalization and extraction of region of interest. The matching scores are generated in two parallel stages: (i) hierarchical matching score from the four topologies of triangulation in the binarized vein structures and (ii) from the geometrical features consisting of knuckle point perimeter distances in the acquired images. The weighted score level combination from these two matching scores are used to authenticate the individuals. The achieved experimental results from the proposed system using contactless palm dorsal-hand vein images are promising (equal error rate of 1.14%) and suggest more user friendly alternative for user identification.

Index Terms—Contact free hand recognition, hand shape, hand vein, palm dorsal vein, vascular biometrics.

I. INTRODUCTION

THE rapid growth in the use of e-commerce applications requires reliable user identification for effective and secure access control. The face identification beyond visible spectrum is increasing receiving attention and has highest user acceptance [7], [23]. Hand vein identification has emerged as a promising component of biometrics study. The subcutaneous vascular pattern/network appearing on the back of hand, referred to as the hand vein in this paper, is extremely difficult to forge and, therefore, offers promising biometric which also ensures liveness. Fig. 1 illustrates the generic vascular map found on the dorsum of the hand. There are mainly two types of hand veins found on the dorsum of the hand, namely *cephalic* and *basilic*. The *basilic* veins are the group of veins attached with surface of hand and marked as "2" in Fig. 1. It generally consists of upper limb of the back of hand. *Cephalic* veins are the group of veins attached with the elbow of the hand and marked as "1" in Fig. 1. The vascular system extends or shrinks with the respective changes in the body. The shape of hand veins changes with the change in the length of body from childhood. In general, no major growth takes place in the adult life and, hence, vein patterns are quite
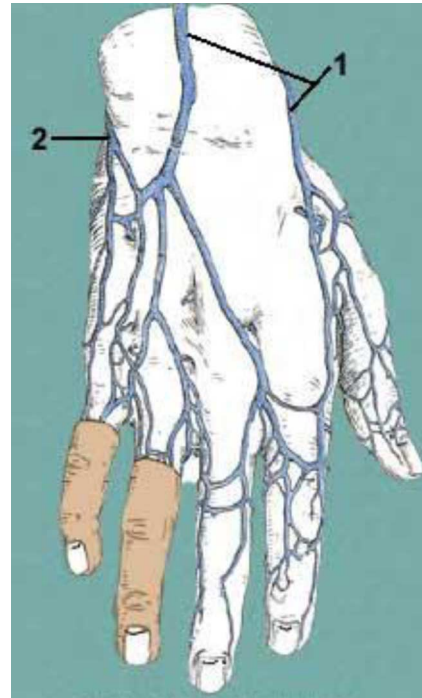
Fig. 1. Example of the generic vascular map on the palm dorsal surface (courtesy of [24]).

stable in the age group of 20–50. After that the vascular system begins to shrink with the decline in the strength of bones and muscles. These changes in vascular system make the vein pattern loose and change its size as compared to earlier. As the vascular system is a large and essential system of the body, it is largely affected due to any change in body, either by nature or by disease. Diabetes, hypertension, atherosclerosis, metabolic disorders [25], and tumors [26] are some diseases which affect the vascular systems and made it thick or thin. There have been several other efforts to investigate the utility of hand vein patterns for effective user authentication. In the following section, we present a brief review on the related prior work which is followed by the salient features of the proposed approach investigated in this paper.

A. Prior Work

The stability and uniqueness of hand vein patterns have attracted the attention of researchers for its usage in the personal identification. The thermal imaging of palm dorsal surfaces typically captures the thermal pattern generated from the flow of (hot) blood in *cephalic* and *basilic* veins. Lin and Fan [1] have
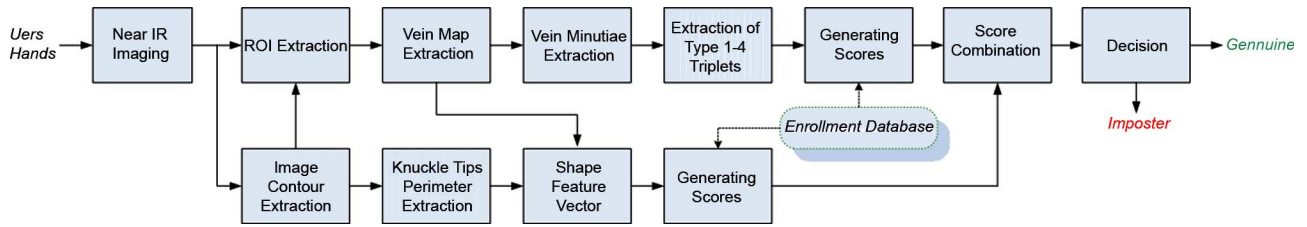
Fig. 2. Block diagram of the personal authentication using near IR hand vein images.

investigated the personal verification from such palm dorsal images acquired from the thermal infrared (IR) camera operating in $(3.4 - 5)$ μ m range. The approach detailed in [1] is fully automated and uses the combination of multiresolution representations from the post processed thermal vein patterns. Wang and Leedham [2] present yet another approach for personal authentication using hand vein images acquired from the thermal imaging. Authors [2], [22] have employed Hausdorff distance to generate matching scores between the extracted line patterns and illustrated promising results.

The subcutaneous blood vessels absorb less radiation, in near IR (780–1100 nm) illumination, than its surrounding blood and, therefore, generates high contrast in the acquired images. Such near IR imaging of hand vein patterns have also been investigated in the literature for personal identification. Cross and Smith [3] have detailed the usage of near IR imaging for the extraction of hand vein patterns. Authors have demonstrated the two-fold matching of medial axis representation, following the vein skeleton extraction, for the authentication of 20 users. Im *et al.* [4], [5] have presented the implementation for hand vein extractor, using FPGA in [4] and DSP processor in [5], but with little details on the matching strategy or on the size/nature of database employed for the performance evaluation. Tanaka and Kubo [8] also developed hand vein acquisition device using near IR imaging and employed FFT based phase correlation scheme for user verification. Recently, some commercial products, e.g., [36], [37], that authenticate individuals from hand veins images are also available. Personal authentication using conjunctival vasculature pattern has been reported in [38].

It is widely known that the thermal (far IR) imaging cameras are highly sensitive to ambient conditions and very expensive. Therefore, the researchers [4], [5], [8], [10] have focused on the solutions using near IR imaging. The imaging setup in prior work [3], [4], [8], [13], [14] employed hand docking frame device (to restrict the translational and rotational changes) which are often inconvenient and not user friendly. Furthermore, with the notable exception of [1], [3], there is no systematic (completely automated) proposal for hand vein based user authentication.

B. Proposed System

In this paper, we develop a new hand vein authentication approach utilizing the structural similarity of hand vein triangulation and knuckle shape features. The block diagram of the proposed approach is shown in Fig. 2. The approach has been adapted to utilize palm dorsal images acquired from the, low-cost, contactless, near IR imaging. The main contributions from this paper [33] can be summarized as follows.

(i) In this paper, we investigate the extraction and matching of hand vein structure using the key point triangulation. It many be noted that the low quality (visibility and clarity) of vein images does not guarantee same number of key points (from same user) and, therefore, a weighted combination of four different types of triangulation is developed. Further details of this strategy can be seen Section VII.

(ii) The proposed method also investigates the utility of knuckle shape features since these features can be simultaneously extracted from the acquired images. The matching scores computed from these knuckle shape features are employed to further improve the performance for the hand vein authentication.

(iii) The usefulness of the proposed method is investigated from the experimental results on the real hand vein images acquired using contactless near infrared imaging. The contactless imaging is expected to yield higher image variations. Therefore, the steps of image normalization and feature extraction have been adapted to reduce the variations in the interclass matching scores.

The image contours extracted from the acquired images are used for the image normalization and segmentation of region of interest (ROI) which is detailed in Sections II–IV. The automated extraction of hand vein map from ROI images is described in Section V. The extraction and triangulation of local key points from the hand vain map is detailed in Sections VI and VII respectively. The hierarchical matching scheme for the triplets is introduced in Section VIII. The experiments and results from this work are presented in Section IX which is followed by the discussion in Section X and the main conclusions from this paper are summarized Section XI.

II. IMAGE ACQUISITION

The acquisition of hand vein images using near IR imaging has been studied in [3], [11], and [15]. In this work, a low-cost near IR camera, traditionally used for surveillance, was employed for the contactless image acquisition. The near IR illumination (LEDs) is evenly and circularly located around the camera and peaks at 850 nm wavelength.[1] The employed near IR camera [12] is fixed at the base and shown in Fig. 3(a). The expected distance between the user hand and the camera was experimentally fixed to 21 cm for the best case acquisition. The volunteers were requested to present their folded right hand (palm dorsal surface) near the imaging window such that the knuckle tip from the middle finger remains at the top. The

---

[1]This wavelength lies in the *medical spectral window* (700–900 nm) in which the illumination penetrates deeper into the tissues [17].
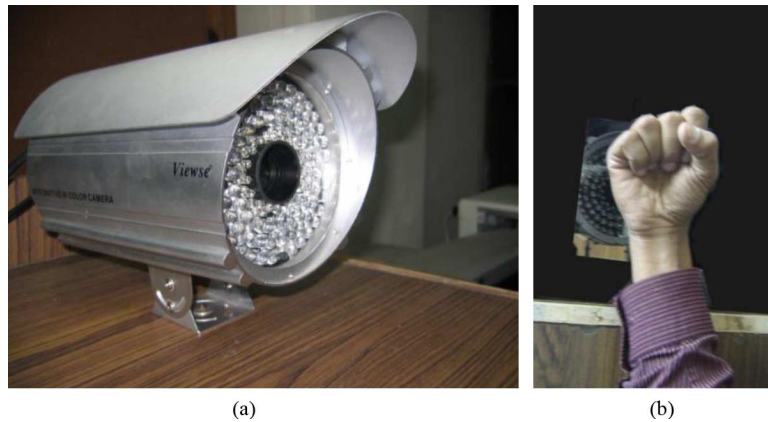
(a) (b)

Fig. 3. Image acquisition setup: (a) employed near IR camera, (b) contactless image acquisition.
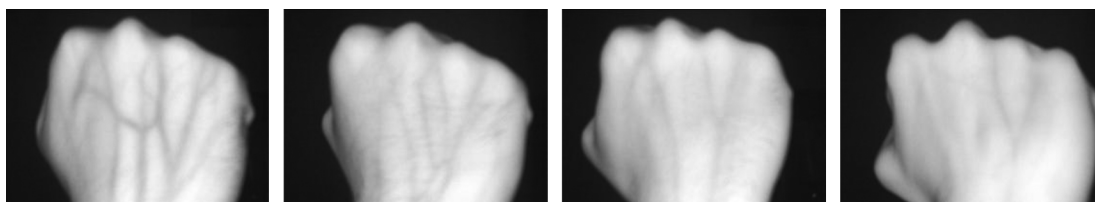

Fig. 4. Samples of the acquired hand vein images.

acquisition of a typical contactless hand vein image is shown in Fig. 3(b). Some of the image samples acquired from our imaging setup are reproduced in Fig. 4.

The incident near-infrared illumination travelling in the palm dorsal skin is absorbed by the haemoglobin in the blood and branches of artery and vein. In addition to the different absorption coefficients, the scattering coefficients of blood and bio-tissue for near infrared illumination are significantly different [34]. The higher scattering coefficient of the blood ensures that more incident infrared illumination changes its path in blood than in the surrounding tissue. It is scattering rather than absorption that dominates and results in the darker appearance of dorsal vein patterns. The Fig. 5 shows representative samples of gray level vein profiles along the direction perpendicular to their length. It can be observed from this figure that these vein profiles are quite noisy and do not have any ideal step edge to distinguish from the background. Although these intensity patterns varies from vein to vein, their average profile can be approximated as Gaussian. The widths of these vein profiles are found in the range of 30–50 pixels. The edge point of vein patterns can be detected by locating zero crossings of second derivative gray level profiles. However, the derivative filters are very sensitive to the accompanying noise (Fig. 5). Therefore, it is judicious to employ some preprocessing, such as averaging, to reduce the effect of noise. This two step process (Laplacian of Gaussian) was found to be quite effective for the localization of venous structure in the acquired hand vein images.

III. EXTRACTION OF KNUCKLE TIPS

The acquired images are firstly binarized using Otsu's thresholding and its contour is obtained as shown in Fig. 6(a). One of the key tasks in image normalization is to obtain reliable control points from the image that can be used for alignment and
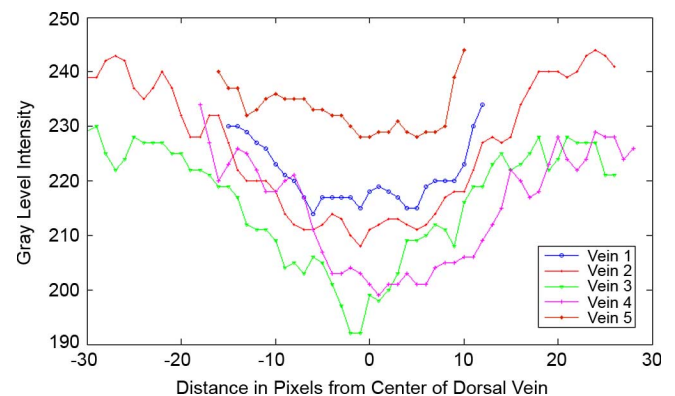

Fig. 5. Gray-level profiles of the cross section of blood vessels in Fig. 4 (first image).

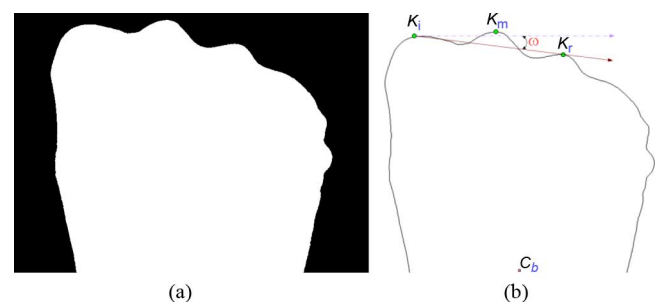

(a) (b)

Fig. 6. (a) Acquired image after thresholding and (b) corresponding contour image with extracted key points for the normalization.

extraction of region of interest (ROI). In our approach, we selected knuckle tips as the control points. The knuckle tips can be easily extracted by locating the peaks in the distance from of every contour point from the middle base point C_b, similar
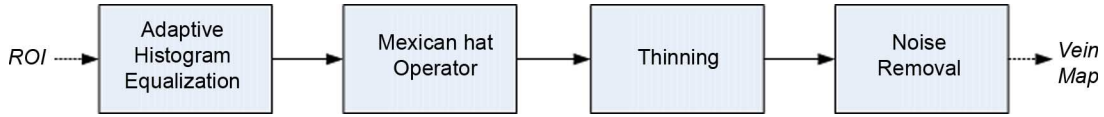
Fig. 7. Extraction of hand vein map from the region of interest images.

to the method used for locating finger tips in the hand geometry identification [19], [20]. Another simpler method is to scan the contour image from left to right and from top to bottom. The point where the first transition occurs from white to black pixel is the first knuckle tip K_m. Similar scanning of the two portions of the image, i.e., left side and right side of K_m, can locate index finger tip (K_i) and ring finger tip (K_r). However, as can be observed from Figs. 4 and 6 (or other images in this paper), the little finger knuckle tip (say K_l) is usually not visible and difficult to locate. In our implementation, the point K_l is approximated contour point at the same row and column distance, as between K_m and K_r, from knuckle tip K_r but from the aligned image contour.

IV. EXTRACTION OF REGION OF INTEREST

Once the key control points (K_i, K_m, K_r) are located, the image orientation is firstly ascertained to extract reliable region of interest. The angle ω, as shown in Fig. 6(b), is first computed. The rotation matrix Ω is used to achieve the vertical alignment of the region of interest, from each of the acquired image, as follows:

$$
\Omega = \begin{bmatrix} \cos(\omega) - \sin(\omega) \\ \sin(\omega)\cos(\omega) \end{bmatrix}
$$
$$
\omega = \tan^{-1}\left\{ \frac{K_r(y) - K_i(y)}{K_r(x) - K_i(x)} \right\} \tag{1}
$$

where (x, y) represents the corresponding coordinates of knuckle tips. Once the alignment angle is estimated, a fixed region of interest (ROI) of size 400×300 pixels is extracted. The size and position of this region is empirically selected and fixed at 150 pixels below K_m and along the line joining K_i and K_r

V. EXTRACTION OF VEIN STRUCTURE

The topological structure of vein patterns is extracted from the segmented region of interest. The images acquired from the low-cost near IR camera are of poor quality and contains obscure parts of veins, mainly due to noise and uneven illumination profile of near IR illuminators fixed at distance. Therefore, the method of vein pattern extraction is empirically tailored to the nature of acquired images and is summarized in Fig. 7. First, the images are subjected to adaptive histogram equalization for image enhancement using local gray level information. The enhanced images are further processed using Laplacian of Gaussian (LOG) or Mexican hat operator

$$
\nabla^2 G_\sigma(x, y) = -\frac{1}{\pi\sigma^4}\left\{ 1 - \frac{x^2 + y^2}{2\sigma^2} \right\} e^{-(x^2 + y^2)/2\sigma^2}. \tag{2}
$$

The LOG operator $\nabla^2 G_\sigma(x, y)$ is employed to identify the image regions with rapid intensity changes while suppressing the noise. The resulting image is subjected to thinning which

generates the vein pattern structure. However, the resulting binary pattern also contains noise, i.e., isolated regions with small connectivity. Therefore, the isolated regions with small (empirically determined threshold) amount of connectivity are eliminated from the thinned hand vein pattern images.

VI. EXTRACTION OF VEIN BIFURCATIOIN AND VEIN ENDINGS

The individuality of vein structure is exclusively determined from the relationship among the local vein characteristics. Therefore, the extracted vein pattern is firstly used to locate the key points that are relatively stable, unique and repeatable. The vein bifurcation and endings points are selected as key points to extract local vein properties. A vein bifurcation is defined as vein point where vein forks or diverges into branch veins, and the vein ending is the point at which vein ends or disappears abruptly. This disappearance could be due to the abrupt ending of blood vessels (as shown in Fig. 1) or their poor visibility from the imaging system. In order to extract the vein endings and bifurcation points we examining the connectivity of every pixel and determine the crossing number $R(\mathbf{m})$ [16] for every pixel $\mathbf{m}$. The crossing number $R(\mathbf{m})$ is the sum of differences between pairs of adjacent pixels in 3×3 window centered at $\mathbf{m}$

$$
R(m) = \sum_{z=1}^{8} |val(\mathbf{m}_{z\bmod 8}) - val(\mathbf{m}_{z-1})|. \tag{3}
$$

The pixel $\mathbf{m}$ with $val(\mathbf{m}) = 1$ corresponds to vein ending point if $R(\mathbf{m}) = 2$, and corresponds to vein bifurcation point if $R(\mathbf{m}) \geq 6$.

VII. FEATURE EXTRACTION USING MINUTIAE TRIANGULATION

The feature extraction approach is to use unique topological structure from the hand vein minutiae using Delaunay triangulation [21]. A minutiae M_i can be represented by its position and type, i.e., $M_i = (p_i, q_i, m_i)$ where (p_i, q_i) denotes the position and m_i denotes the type of minutiae (vein bifurcation or endings). The idea is to extract meaningful minutiae groups, i.e., triplets or triangles, from the hand vein map to achieve rotation and translation invariant representation of local information. Given a minutiae triangle (Fig. 8), we separately compute three lengths λ_1, λ_2, and λ_3. Then all the sides of triangle are sorted to avoid considering all possible orders of same lengths

$$
\lambda_1 \geq \lambda_2 \geq \lambda_3. \tag{4}
$$

A 4-D index $(\varepsilon_j, \lambda_1, \lambda_2, \lambda_3)$ with $\varepsilon_j = 1, 2, 3, 4$, is formed by indexing the triplets in the vein map. As shown in Table I, we considered four types of triplets, i.e., ε_j, depending on the combinations of three types of minutiae. The number of minutiae points that can be extracted from the low quality ROI images is limited. In addition, the matching strategy should also accommodate missing and spurious minutiae points. We consider that
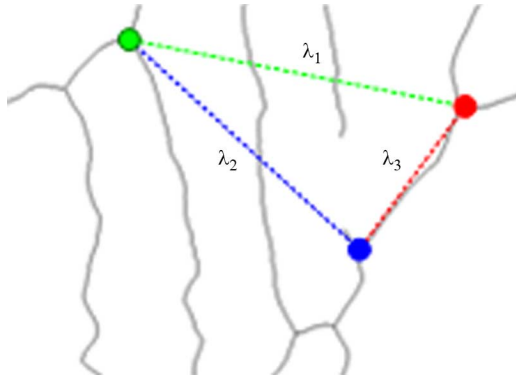
Fig. 8. Selection of a triplet (type 1) from the extracted hand vein map.

TABLE I
HIERARCHAL CLASSIFICATION OF TRIPLET TYPES.

Triplet Type	Minutiae Type*		
ε_j	m_1	m_2	m_3
1	b	b	b
2	b	b	e
3	b	e	e
4	e	e	e

*b – bifurcation, e- ending

two triplets Y and Y' are matched only if they satisfy the following set of conditions:

$$\varepsilon_j = \varepsilon'_j, |\lambda_1 - \lambda'_1| < T_m, |\lambda_2 - \lambda'_2| < T_m$$
$$|\lambda_3 - \lambda'_3| < T_m. \quad (5)$$

The threshold T_m can be empirically selected depending on the image size and quality.

VIII. SCORE ASSIGNMENT

Once the extracted triplets are matched, using the criteria in (5), the matching scores are assigned. The score assignment scheme is hierarchical and assigns higher scores to more likely true matches. If two triplets having three bifurcation points, i.e., type 1, are matched then there is higher probability that they corresponds to the same user vein map. Therefore, such matches are assigned higher scores. However, those matching triplets formed due to three vein endings, i.e., type 4, have small probability/reliability that they have originated from the vein map of the same user. Our observationshave suggested that the chances of spurious vein ending formation (due to image quality or vein extraction process) in vein map are higher. Therefore, the score assignment for such matched triplets is the lowest (Fig. 9). The weights (or scores) are experimentally determined and such that $w_1 > w_2 > w_3 > w_4$. Thus, each of the matched triplet type is assigned a score and the cumulative matching score (s_c) from all the matched triplet types is computed for every pair of hand vein matching. In addition to the usage of matching scores from the vein map (as discussed above), we also investigate the usefulness of additional features that are simultaneously extracted from the acquired images. The perimeter of pixels between four knuckle tips $(K_i, K_m, K_r,$ and $K_l)$ from the normalized contour image is computed. Thus, three contour distances, say $p_1, p_2,$
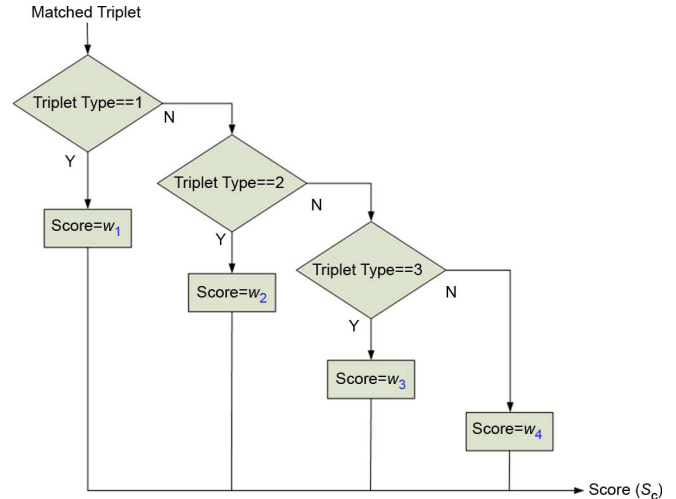

Fig. 9. Score generation from a matched triplet.

p_3 corresponding to distance between knuckle points $K_i - K_m$, $K_m - K_r$, $K_r - K_l$, respectively, are also used as features. In addition, the perimeter of vein map (extracted as detailed in Section V, Fig. 7), i.e., number of white or on pixels (p_4) are also used for the characterization of vein shape. Thus, four features $(p_1 - p_4)$ are used to form separate shape feature vector. The Euclidean distance between two shape features, from the two hand vein images, is used as shape matching score (s_g). The weighted combination of two matching scores, s_c and s_g, is used compute a single consolidated matching score [35]. These consolidated matching scores are used to assign class labels (genuine or imposter) using the decision threshold.

IX. EXPERIMENTS AND RESULTS

The performance of the proposed authentication scheme was evaluated on hand vein database acquired in the real environment. This database mainly consisted of the right hand vein images collected from the students and staff in our university. The database from the 100 users, with three images per user, was acquired during October 2006 to May 2007. All the subjects in the database are in the age group 14–55 years comprising of 81 males and 19 females. The imaging setup has been detailed in Section II and the size of each of the acquired images was 768×576 pixels. The peg-free imaging introduces scale changes as it is very unlikely that user presents his/her hand at the same distance during successive imaging. In addition, the acquired images also had rotational intraclass variations. Some volunteers were not very cooperative and none of them were paid for the imaging.

The ROI extraction steps detailed in Sections III and IV were employed to extract 400×300 pixels size ROI images. These images were used to extract vein map as detailed in Section V. The standard deviation of the 60×60 Mexican hat operator was empirically fixed to 0.25. The contrast limited adaptive histogram equalization was performed on 9×9 subregions and matched to Rayleigh distribution with the variance of 9. All the isolated regions with 8 connected pixels and less than 100 counts were removed from the thinned images (noise removal step in Fig. 7). Figs. 10 and 11 show samples from the acquired images,
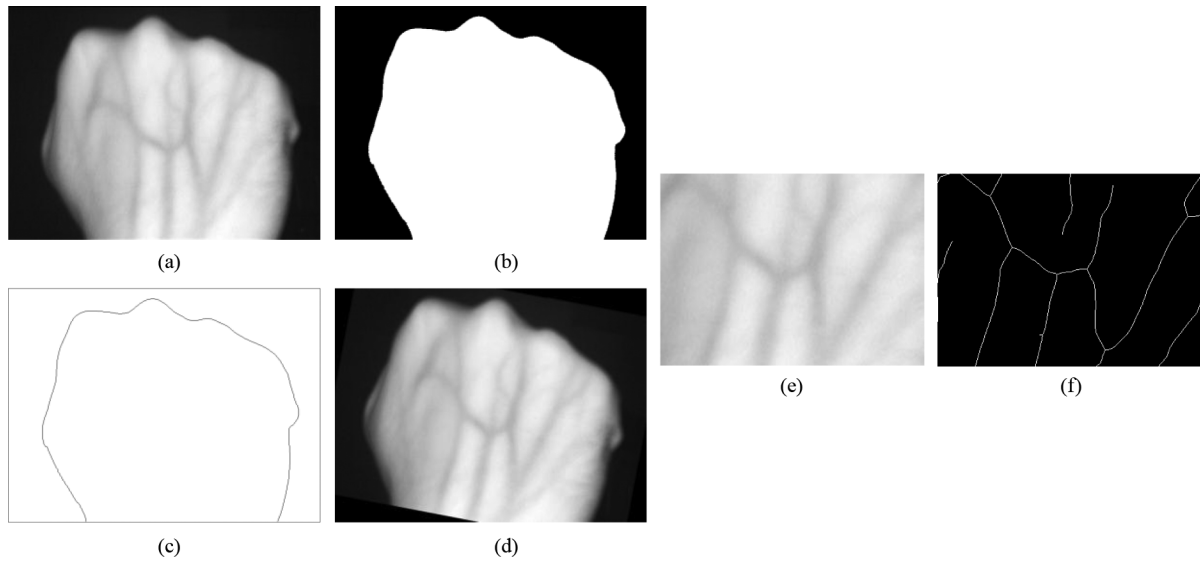
Fig. 10. Extraction of vein topology: (a) acquired hand images, (b) binarized image, (c) hand contour, (d) normalized image, (e) extracted region of interest, and (f) extracted hand-vein topology.
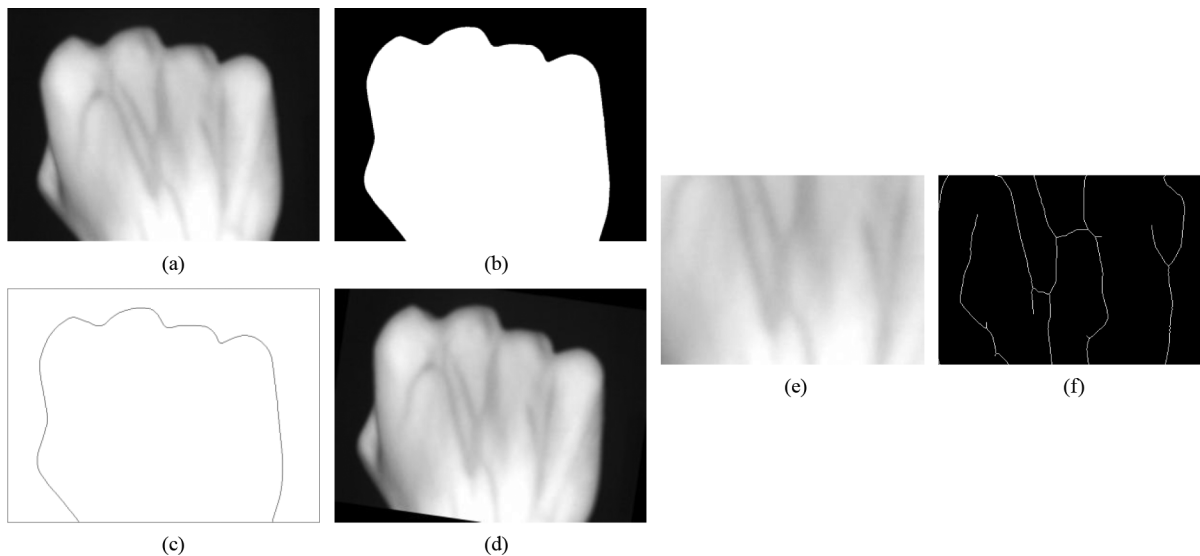

Fig. 11. Extraction of vein topology: (a) acquired hand images, (b) binarized image, (c) hand contour, (d) normalized image, (e) extracted region of interest, and (f) extracted hand-vein topology.

corresponding normalized images, extracted region of interest and their respective vein map. The number of vein bifurcation points that can be extracted from the acquired images (region of interest) never exceeded 10. However, the matching scheme detailed in Section VII has been adapted to handle the spurious vein endings. The weights from different triplet types were empirically selected as 40, 15, 8, 3 corresponding to w_1, w_2, w_3 and w_4, respectively. The experimental results reported in this paper employed two images for the training and rest one to ascertain the test performance for the user authentication. However, this was repeated and the average performance from the three different test set is reported. We firstly evaluated the performance from matching scores using (s_c) which was generated from the triplet matches. Then the performance from the geometrical features obtained from the knuckle tip distances, i.e., matching scores s_g, was integrated to ascertain the perfor-

mance improvement. The weights for the combination of two matching scores, s_c and s_g, were empirically selected as 0.8 and 0.2, respectively. The distribution of genuine and imposter scores obtained from the triplet matches and from the geometrical features is shown in Fig. 12. The receiver operating characteristics from the test data for the average performance is shown in Fig. 13. The performance from the usage of knuckle tip distances is very low. However, the performance improvement due to the integration of these features is significant and can be observed from the same figure. Fig. 14 shows the variation of the False Acceptance Rate (FAR) and False Reject Rate (FRR) with the decision threshold, corresponding to the combined matching scores. The equal error rate from the matching scores due to triplets alone (s_c) is 1.77%. The equal error rate of 1.14% was achieved from the combined matching scores which can also be seen from Fig. 14.
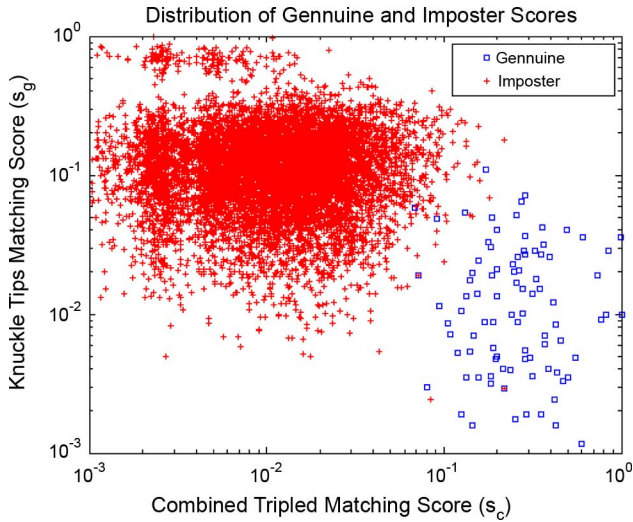
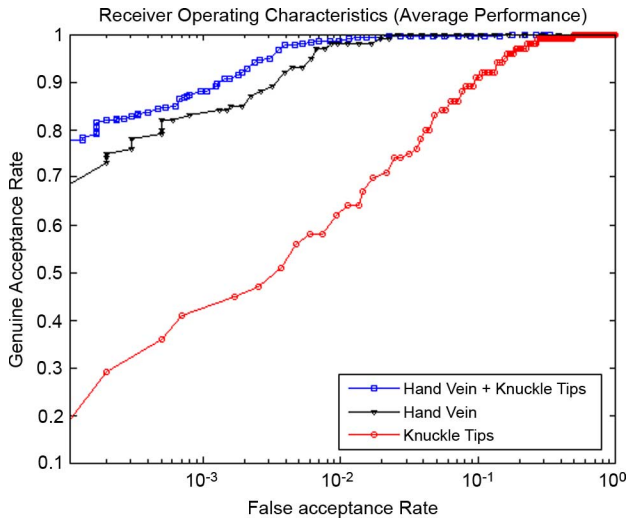Fig. 12. Distribution of genuine and imposter matching scores.

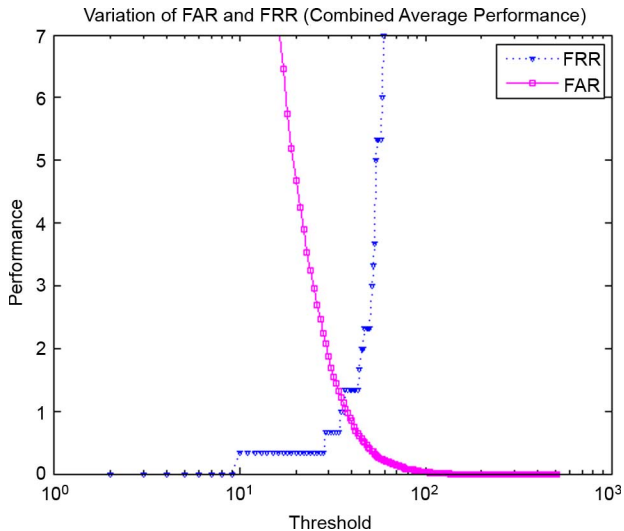Fig. 13. ROC for the average performance from the test image samples.

Fig. 14. Variation of FAR and FRR with decision threshold (combined performance).

Fig. 15(a) shows the distribution of combined triplet matching scores obtained from the palm dorsal veins for the genuine user comparisons. Similarly, the distribution of genuine user comparison scores obtained from the knuckle tip distances is shown in Fig. 15(b). The statistical estimation of confidence level for the biometric authentication requires an excellent match between the theoretical distribution and the real score distribution. Therefore, Figs. 15(a) and (b) also illustrates the best fit statistical model obtained for the corresponding score distributions using generalized extreme value distribution. The preference of generalized extreme value (GEV) distribution to model the distribution of real world data has been illustrated in several [29], [30]. The GEV distribution was also found to be most appropriate, i.e., best fit, to model the matching score distributions from our experiments. The GEV (μ, α, τ) distribution, for the matching score probability s, is characterized by three parameters; μ, α, and τ representing location, scale and shape respectively. The probability distribution of GEV distribution is characterized as follows:

$$f(s_i|\tau, \mu, \alpha) = \frac{1}{\alpha} \exp\left(-\left(1 + \tau \frac{(s - \mu)}{\alpha}\right)^{-1/\tau}\right)$$

$$\times \left(1 + \tau \frac{(s - \mu)}{\alpha}\right)^{-1-1/\tau} \text{ for } 1 + \tau \frac{(s - \mu)}{\alpha} > 0. \quad (6)$$

The more details on GEV distribution can be found in [29]. Daugman [31] has presented an optimal method for iris representation based on the distribution of a Hamming distances from the irisCode. The binary nature of outcomes from the imposter matching decisions suggests that the Binomial distribution can be more appropriate model for analyzing the distribution of a Hamming distances, generated from the optimal method of iris representation. Instead, the distribution of such matching scores from the palm dorsal veins employed in our work closely follow GEV distribution (Figs. 15 and 16) and suggests its preference (over Binomial or Gaussian) to model the theoretical distribution of matching scores.

X. DISCUSSION

The clarity and visibility of subcutaneous blood vessels varies across the user population and depends on the physiological variations, ambient temperature, humidity, hand pose, health and thickness of subcutaneous fat layer. The variation in the size and structure of venous components (e.g., lipid membrane, collagen fibres and nuclei) affect its scattering properties and alters the distribution of photon flux [28]. In addition, the clarity of palm dorsal veins in the acquired images is also influenced by the presence of hairs, moles and scars on skin surface and also its pigmentation. Therefore, the investigated approach for the personal authentication does not depend only on the topology of venous network but also on the skin pigmentation and fat depositions on the dorsum of hand. The poor visibility of veins in the acquired images results in inaccurate extraction of venous structure and can generate spurious or missing minutiae points, which degrades the performance of the system.

The average number of minutiae that that can be extracted from the low quality, i.e., poor vascular visibility and clarity,
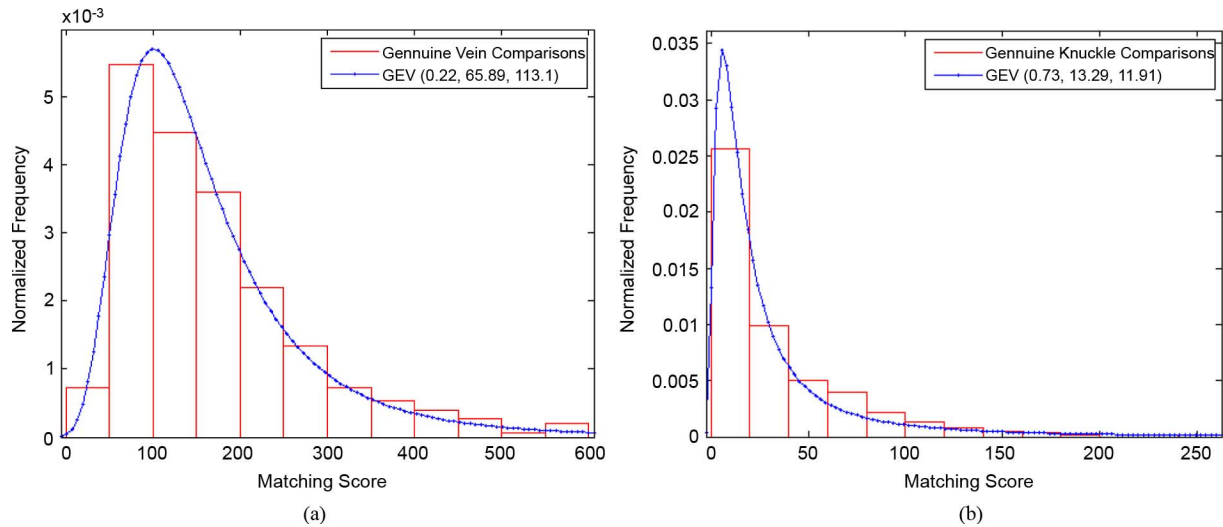
Fig. 15.   Estimation of theoretical distribution from (a) genuine vein matching scores and (b) genuine knuckle matching scores.
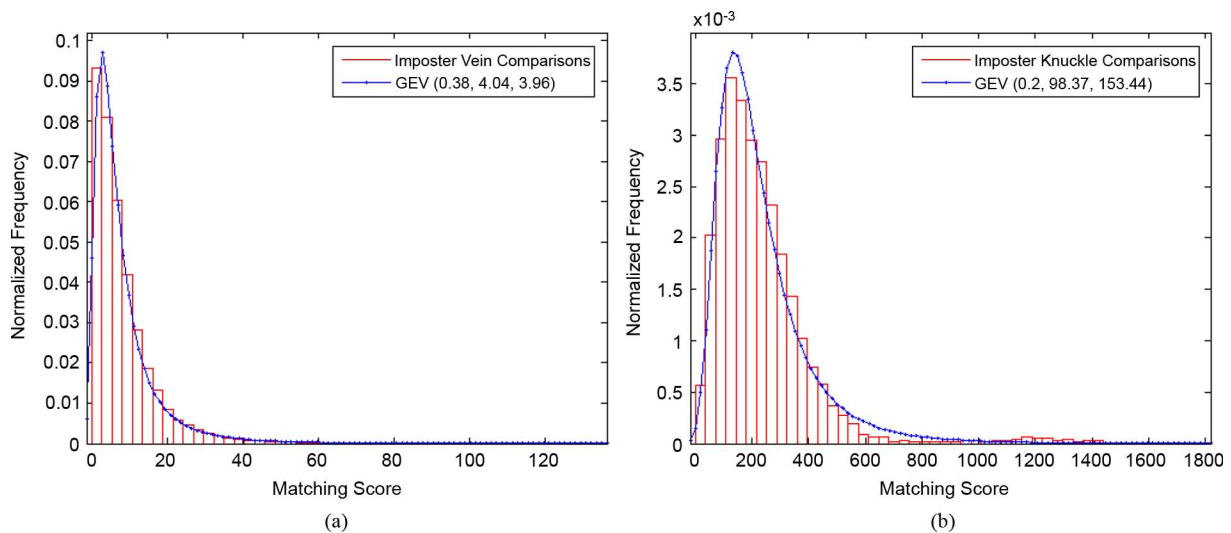

Fig. 16.   Estimation of theortical distribution from (a) imposter vein matching scores and (b) imposter knuckle matching scores.

images were limited. It is interesting to note that the average number of ridge bifurcations extracted per image from our experiments was 2.81 while the average number of ridge endings observed per image was 11.53. Although the average number of ridge endings is expected to be higher than ridge bifurcations, the effect of associated noise in acquired images was observed to be more pronounced in generating spurious ridge endings than spurious bifurcations. The average number of triplets (Table I) of type 1, 2, 3, and 4 per image from our experiments were 1.53, 7.32, 12.84, and 119.82, respectively. The selection of threshold T_m in (5) is a judicious compromise between two key considerations. The larger values of threshold T_m requires large number of triplets to be matched and, therefore, increases the computational complexity. On the other hand, smaller values of T_m are also not desirable as they limit the genuine matches from the hand vein images with nonlocal deformations.

XI. CONCLUSION

This paper has proposed a new approach for the hand authentication using vein triangulation. In addition, the unique knuckle

point perimeter distances were also simultaneously extracted from the same image and utilized to achieve the performance improvement. The utility of knuckle shape biometric has been cited in [9] but there has been negligible attention on its usage in the biometric literature [18]. The experimental results illustrated in previous section, i.e., equal error rate of 1.14% on the database of 100 users, are certainly promising. The illustrated performance should be interpreted in the context of contactless imaging as such images are expected to present higher intraclass variations as compared to those acquired from fixed imaging using hand docking devices. Table II presents comparative summary of prior work on the hand vein (back surface) authentication approaches presented in the literature.

This table suggests that the prior approaches have employed small size database but also achieved promising results. The contactless imaging is perceived to be more hygienic and user friendly but it poses problems of missing or spurious vein minutiae points. This is mainly due to the resulting uneven illumination and the fact that the palm back surface is 3-D curved surface. The hierarchical weighting of triplets is,

TABLE II
COMPARATIVE SUMMARY OF RELATED WORK ON HAND VEIN (BACK SURFACE) BASED AUTHENTICATION

Reference	Methodology	Imaging	Database	Performance
T. Tanaka and N. Kubo [8]	FFT based phase correlation	Near Infra Red, HDF	25 Users	FAR – 0.73% FRR – 4%
C.-L. Lin and K.C. Fan [1]	Multi-resolution analysis and combination	Thermal Hand Vein Imaging (3.4-5 μm)	32 Users	FAR - 1.5% FRR - 3.5%
L. Wang and G. Leedham [2]	Line segment Hausdorff distance matching	Thermal Hand Vein Imaging (8-14 μm)	12 Users	FAR – 0 % FRR – 0%
Y. Ding, D. Zhuang and K. Wang [13]	Distance between feature points	Near IR Imaging, HDF	48 Users	FAR – 0 % FRR - 0.9%
J. M. Cross and C. L. Smith [3]	Sequential Correlation in vein maps	Near IR Imaging, HDF	20 Users	FAR – 0 % FRR - 7.9%
This Paper	Matching vein triangulation and shape features	Near IR Imaging, Contactless	100 Users	FAR - 1.14% FRR - 1.14%

* HDF – Hand Docking Frame

therefore, suggested to achieve better matching performance from such images. The imaging setup employed in our work has been developed for the cooperative users in the indoor environment. It makes an assumption that user is keen to authenticate himself/herself for access and not yet suitable for the uncooperative user. The strong near IR component present in the sunlight also limits the usage of employed imaging setup for outdoor usage. The background during the indoor imaging can be controlled and can be conveniently made uniform. Our current imaging setup employs fixed focus and cannot accommodate large changes in the imaging distance. However, inclusion of auto-focus in the imaging setup, similar to as employed in [32] for iris imaging, can help to accommodate large changes in the imaging distance/scale. *Although more work remains to be done, our results to date indicate that the combination of hand vein and knuckle shape features constitutes a promising addition to the biometrics based personal authentication.* It is encouraging that the performance from such palm-dorsal images, using unconstrained and low-cost image setup, compares very well (or better) with the hand-geometry biometric which is has very high user acceptance [18]. While hand-geometry biometric is highly prone to spoofing, vascular biometric like palm dorsum vein are extremely difficult to forge and at the same time have high user acceptance for its deployment in civilian applications. Further improvement in the performance of proposed system, that simultaneously combines knuckle shape and dorsal vein features, using auto-focus and more sensitive near infrared camera is expected and requires further investigation. The discretization of noisy biometric features has been recently shown to offer significant improvement in the performance. This is especially useful for low-resolution imaging, such as hand geometry or the hand vein employed in this work, and is suggested for further work.

REFERENCES

[1] C.-L. Lin and K.-C. Fan, "Biometric verification using thermal images of palm-dorsa vein patterns," *IEEE Trans. Circuits Syst. Video Technol.*, vol. 14, no. 2, pp. 199–213, Feb. 2004.

[2] L. Wang and G. Leedham, "A thermal hand-vein pattern verification system," in *Pattern Recognition and Image Analysis*, S. Singh, M. Singh, C. Apte, and P. Perner, Eds. New York: Springer, 2005, vol. 3687, pp. 58–65.

[3] J. M. Cross and C. L. Smith, "Thermo graphic imaging of the subcutaneous vascular network of the back of the hand for biometric identification," in *Proc. IEEE 29th Annu. Int. Carnahan Conf. Security Technology*, Sander-Stead, Surrey, U.K., Oct. 1995, pp. 20–35.

[4] S.-K. Im, H.-M. Park, S.-W. Kim, C.-K. Chung, and H.-S. Choi, "Improved vein pattern extracting algorithm and its implementation," in *Proc. Int. Conf. Consumer Electronics*, Jun. 2000, pp. 2–3.

[5] S. K. Im, H. M. Park, Y. W. Kim, S. C. Han, S. W. Kim, and C. H. Hang, "An biometric identification system by extracting hand vein patterns," *J. Korean Phys. Soc.*, vol. 38, pp. 268–272, Mar. 2001.

[6] J. Mehnert, J. M. Cross, and C. L. Smith, "Thermal graphic imaging: Segmentation of the subcutaneous vascular network of the back of the hand," Research Rep., Edith Cowan Univ., Australian Inst. Security Appl. Technol., Perth, Western Australia, 1993.

[7] S. Z. Li, R. Chu, S. Liao, and L. Zhang, "Illumination invariant face recognition using near-infrared images," *IEEE. Tran. Pattern Anal. Mach. Intell.*, vol. 29, no. 4, pp. 627–639, Apr. 2007.

[8] T. Tanaka and N. Kubo, "Biometric authentication by hand vein patterns," in *Proc. SICE Annu. Conf.*, Yokohama, Japan, Aug. 2004, pp. 249–253.

[9] C. Colbert, "Knuckle Profile Identity Verification System," U.S. Patent, 5,862,246, Jan. 1999.

[10] G. T. Park, S. K. Im, and H. S. Choi, "A person identification algorithm utilizing hand vein pattern," in *Proc. Korea Signal Processing Conf.*, 1997, vol. 10, pp. 1107–1110.

[11] S. Zhao, Y. Wang, and Y. Wang, "Biometric verification by extracting hand vein patterns from low-quality images," in *Proc. 4th ICIG*, Aug. 2007, pp. 667–671.

[12] [Online]. Available: http://www.viewse.com.cn/ProductOne.asp?ID= 106

[13] Y. Ding, D. Zhuang, and K. Wang, "A study of hand vein recognition method," in *Proc. IEEE Int. Conf. Mechatronics & Automation*, Niagara Falls, Canada, Jul. 2005, pp. 2106–2110.

[14] K. Wang, Y. Zhang, Z. Yuan, and D. Zhuang, "Hand vein recognition based on multi supplemental features of multi-classifier fusion decision," in *Proc. IEEE Intl. Conf. Mechatronics Automation*, Luoyang, China, Jun. 2006, pp. 1790–1795.

[15] L. Wang and G. Leedham, "Near- and far-infrared imaging for vein pattern biometrics," in *Proc. IEEE Int. Conf. Video Signal Based Surveillance*, Sydney, Nov. 2006, pp. 52–57.

[16] D. Maltoni, D. Maio, A. K. Jain, and S. Prabhakar, *Handbook of Fingerprint Recognition*.   New York: Springer, 2003.

[17] S. Fantini and M. A. Franceschini, *Handbook of Optical Biomedical Diagnostics*.   Bellingham, WA: SPIE, 2002.

[18] *Handbook of Biometrics*, A. K. Jain, P. Flynn, and A. Ross, Eds.   New York: Springer, 2007.

[19] C. Oden, A. Ercil, and B. Buke, "Combining implicit polynomials and geometric features for hand recognition," *Pattern Recognit. Lett.*, vol. 24, pp. 2145–2152, 2003.

[20] A. Kumar and D. Zhang, "Personal recognition using hand-shape and texture," *IEEE Trans. Image Process.*, vol. 15, no. 8, pp. 2454–2461, Aug. 2006.

[21] G. Bebis, T. Deaconu, and M. Georgiopoulos, "Fingerprint identification using Delaunay triangulation," in *Proc. Int. Conf. Information Intelligence and Systems*, 1999, pp. 452–459.

[22] L. Wang, G. Leedham, and S.-Y. Cho, "Minutiae feature analysis for infrared hand vein pattern biometrics," *Pattern Recognit.*, vol. 41, no. 3, pp. 920–929, 2008.

[23] P. Buddaharaju, I. Pavlidis, P. Tsiamyrtzis, and M. Bazakos, "Physiology-based face recognition in the thermal infrared spectrum," *IEEE. Tran. Pattern Anal. Mach. Intell.*, vol. 29, no. 4, pp. 613–626, Apr. 2007.

[24] W. Norman, The Anatomy Lesson [Online]. Available: http://home.comcast.net/~wnor

[25] O. A. Carretero, "Vascular remodeling and the kallikrein-kinin system," *J. Clin. Invest.*, vol. 115, pp. 588–591, Mar. 2005.

[26] P. Carmeliet and R. K. Jain, "Angiogenesis in cancer and other diseases," *Nature*, vol. 407, pp. 249–257, 2000.

[27] J.-G. Wang, W.-Y. Yau, A. Suwandy, and E. Sung, "Person recognition by palmprint and palm vein images based on 'Laplacianpalm' representation," *Pattern Recognit.*, vol. 41, pp. 1531–1544, 2008.

[28] P. S. Pandian, M. Kumaravel, and M. Singh, "Optical imaging and parametric characterization of frostbite changes in human hand tissues," *Current Sci.*, vol. 95, no. 2, pp. 196–203, Jul. 2008.

[29] S. Kotz and S. Nadarajah, *Extreme Value Distributions: Theory and Applications*.   Singapore: World Scientific, 2001.

[30] S. Coles, *An Introduction to Statistical Modeling of Extreme Values*. New York: Springer-Verlag, 2001.

[31] J. Daugman, "The importance of being random: Statistical principles of iris recognition," *Pattern Recognit.*, vol. 36, no. 2, pp. 279–291, 2003.

[32] K. R. Park and J. Kim, "A real-time focusing algorithm for iris recognition camera," *IEEE Trans. Syst. Man Cybern. C*, vol. 35, pp. 441–444, Aug. 2005.

[33] A. Kumar and K. V. Prathyusha, "Personal authentication using hand vein triangulation," in *Proc. SPIE Conf Biometric Technology for Human Identification*, Orlando, FL, Mar. 2008, vol. 6944, p. 69440E-69440E-13.

[34] J. Mobley and T. Vo-Dinh, *Biomedical Photonics Handbook*.   Boca Raton, FL: CRC, 2003.

[35] A. K. Jain, Y. Chen, and M. Demirkus, "Pores and ridges: Fingerprint matching using level 3 features," *IEEE. Tran. Pattern Anal. Mach. Intell.*, vol. 29, no. 1, pp. 15–27, Jan. 2007.

[36] [Online]. Available: http://www.fujitsu.com/global/about/rd/200506 palm-vein.html

[37] [Online]. Available: http://www.bionicsk.co.jp/english/product/va200. html

[38] R. Derakhshani and A. Ross, "Conjunctival Scans for Personal Identification," U.S. Patent 7327860, Feb. 5, 2008.

Ajay Kumar (S'00–M'01–SM'07) received the Ph.D. degree from The University of Hong Kong in May 2001.

He was with the Indian Institute of Technology, Kanpur, as Junior Research Fellow and at Indian Institute of Technology, Delhi, as Senior Scientific Officer before joining Indian Railways. He joined the Indian Railway Service of Signal Engineers (IRSSE) in 1993 and worked as Assistant Signal and Telecom Engineer. He was a Research Associate with The University of Hong Kong from December 1998 to August 1999. He completed his doctoral research at The University of Hong Kong in a record time of 21 months (September 1999 to May 2001). He worked for his postdoctoral research in the Department of Computer Science, Hong Kong University of Science and Technology, from October 2001 to December 2002. He was awarded The Hong Kong Polytechnic University Postdoctoral Fellowship 2003–2005 and worked in the Department of Computing from April 2004 to January 2005. He has been an Assistant Professor in the Department of Electrical Engineering, Indian Institute of Technology, Delhi, since 2005. He is the founder and lab in-charge of Biometrics Research Laboratory at Indian Institute of Technology, Delhi. His research interests include pattern recognition with the emphasis on biometrics and computer-vision based defect detection.

K. Venkata Prathyusha received the B.E. (electronics and communication) degree from SRKR Engineering College, Bhimavaram, India, in 2005.

She joined the Indian Institute of Technology (IIT), Delhi, in 2005, for the M.Tech. degree program at IIT Delhi, New Delhi, India. She has been working in the Biometrics Research Laboratory, Department of Electrical Engineering, in computer technology.